AJNR

Gd-DTPA-enhanced MR imaging of the brain in patients with meningitis: comparison with CT.

K H Chang, M H Han, J K Roh, I O Kim, M C Han and C W Kim

AJNR Am J Neuroradiol 1990, 11 (1) 69-76
http://www.ajnr.org/content/11/1/69

Gd-DTPA–Enhanced MR Imaging of the Brain in Patients with Meningitis: Comparison with CT

Kee Hyun Chang[1]
Moon Hee Han[1]
Jae Kyu Roh[2]
In One Kim[1]
Man Chung Han[1]
Chu-Wan Kim[1]

Plain and Gd-DTPA–enhanced MR images of the brain were obtained in 18 consecutive patients with meningitis (eight with tuberculous, five with bacterial, three with viral, and two with fungal infections); the MR images were compared with CT scans. MR images were obtained on a 2.0-T superconducting unit with both T1- and T2-weighted pulse sequences before injection and with a T1-weighted sequence after injection of Gd-DTPA (0.1 mmol/kg) in all patients. In tuberculous meningitis, MR imaging depicted ischemia/infarct, hemorrhagic infarct of basal ganglia, meningeal enhancement at either basal cistern or convexity surface of brain, and associated small granulomas in a few more patients than CT did. In bacterial meningitis, primary foci of extracranial inflammation (i.e., mastoid, paranasal sinuses) and adjacent intracranial lesions including localized dural inflammation, subdural fluid collection, and/or brain parenchymal lesions were demonstrated much better on MR than on CT. Otherwise, MR images generally matched the CT scan. Although the plain MR images, both T1- and T2-weighted, were the most sensitive in delineating ischemia/infarct, hemorrhage, and edema, they were not as specific as Gd-DTPA–enhanced T1-weighted images and postcontrast CT scans in defining the active inflammatory process of the meninges and focal lesions precisely.

We conclude that if Gd-DTPA is used, MR imaging appears to be superior to CT in the evaluation of patients with suspected meningitis. Precontrast MR is needed to delineate ischemia/infarct, edema, and subacute hemorrhage.

***AJNR* 11:69–76, January/February 1990; *AJR* 154: April 1990**

CT has been used effectively to evaluate the presence or absence of associated inflammatory mass, infarct, and hydrocephalus and the status of an abnormal blood-brain barrier (BBB) in leptomeningeal inflammation [1–4]. In little more than a decade after the introduction of CT, MR imaging has become a valuable clinical tool that has proved to be superior to CT in evaluating many intracranial diseases [5–10]. However, the specific role of MR imaging has not yet been defined in leptomeningitis, even though the MR appearance of intracranial infectious diseases has been described in the literature [8, 10–17]. The purposes of this study were to evaluate the role of MR imaging, to assess the value of Gd-DTPA enhancement, and to discover the special advantages, if any, of MR over CT in the evaluation of meningitis.

Materials and Methods

Eighteen consecutive patients with meningitis (eight tuberculous, five bacterial, two fungal, and three viral) were examined with MR before and after IV injection of Gd-DTPA (Shering AG, Berlin, W. Germany). The 11 male and seven female patients were 12–65 years old. Fully informed consent was obtained in each case. Microbiological confirmation of the diagnosis was available in six patients (three tuberculous, one bacterial, and two cryptococcal meningitis). In the microbiologically unproved cases the diagnosis was established on the basis of other criteria: In five cases of tuberculous meningitis it was based on the CSF profile, coexisting tuberculous infection in another organ, family history of tuberculosis, and the

Received February 3, 1989; revision requested April 5, 1989; revision received May 23, 1989; accepted July 12, 1989.

This work was supported in part by a grant from the special research fund of Seoul National University Hospital (1989).

[1] Department of Diagnostic Radiology, College of Medicine, Seoul National University, Seoul National University Hospital, 28, Yeongun-Dong, Chongro-Ku, Seoul 110-744, Korea. Address reprint requests to K. H. Chang.

[2] Department of Neurology, College of Medicine, Seoul National University, Seoul 110-744, Korea.

0195–6108/90/1101–069

response to antituberculous regimens during the illness. In four patients with meningitis of bacterial origin, the diagnosis was based on the CSF profile, the response to the antibiotics, and the course of the illness. In the three cases of viral meningitis the diagnosis was based on the CSF profile and the short course of the illness without any specific treatment.

MR imaging was performed with a superconducting unit (Spectro-20000, Goldstar, Seoul, Korea) operating at 2.0 T. With a head coil (diameter, 30 cm), all images were produced by using multislice, multiecho spin-echo (SE) pulse sequences and a two-dimensional Fourier transform image reconstruction technique. All patients had precontrast T1-weighted images, 500–600/30/2–4 (TR/TE/excitations); intermediate-weighted images, 3000/30/1; and T2-weighted images, 3000/80/1. After IV injection of Gd-DTPA (0.1 mmol/kg body weight), all patients were studied with T1-weighted images only; however, in an earlier period of the study five patients had intermediate- and T2-weighted images also. The section thickness/gap was 8 mm/2 mm in T1-weighted imaging and 5 mm/1 mm in T2-weighted imaging. As a rule, we chose an axial imaging plane corresponding to that of the CT examination. The images were acquired on a 256 × 256 matrix with spatial resolution of 1 × 1 mm.

Pre- and postcontrast CT scans were obtained 1–13 days before the MR study in all patients. Either a GE CT/T 8800 or 9800 or equivalent third-generation unit was used.

A retrospective comparison was done between MR and CT findings with attention to identification of abnormal meningeal enhancement; parenchymal signal abnormalities including ischemia/infarct, hemorrhage, granuloma, and abscess; hydrocephalus; periventricular edema; and other associated findings. When parenchymal lesions of high signal intensity on T2-weighted images and of iso- or hypointensity on T1-weighted images were observed in the basal ganglia, thalamus, brainstem, or a major vascular territory, they were designated as ischemia/infarct.

Results

Of eight patients with tuberculous meningitis, cisternal obliteration and abnormal enhancement were identified in six patients on MR (Figs. 1–3) and in five on CT. In one patient in whom a disparity was seen between CT and MR, CT could not differentiate between normal and abnormal cisternal enhancement. The most common site of enhancement was the suprasellar cistern; next were the ambient cistern and sylvian fissure. Curvilinear meningeal enhancement along the convexity surface of the brain was noticed in one patient on MR only (Fig. 2). Associated granulomas ranging from 2 to 10 mm

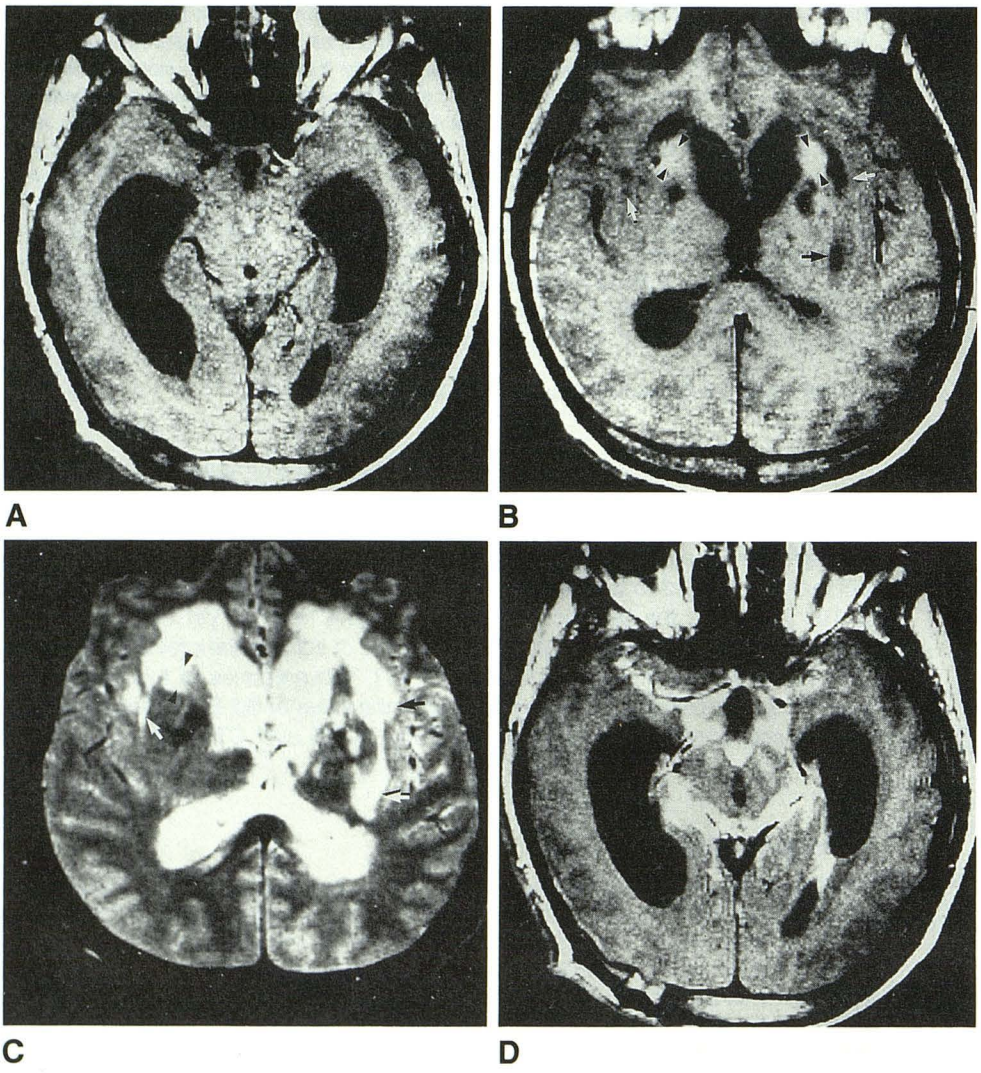

Fig. 1.—Case 1: Tuberculous meningitis.

***A* and *B*, Precontrast SE 500/30 images show obliteration of basal cisterns, hydrocephalus, and ischemia/infarct (*arrows*) with hemorrhagic foci (*arrowheads*) in basal ganglia bilaterally.**

***C*, Precontrast SE 3000/80 image shows multiple areas of high signal intensity mainly representing edema and ischemia/infarct (*arrows*) with hemorrhagic foci (*arrowheads*) in basal ganglia, external capsules, and periventricular white matter bilaterally. Lesions appear to be much more extensive on 3000/80 image than on 500/30 images. Bilateral low signal intensities at globus pallidus seen on *B* and *C* represent calcifications, which were verified on CT (not shown).**

***D*, GD-DTPA–enhanced SE 500/30 image reveals extensive contrast enhancement in suprasellar and perimesencephalic cisterns and left ventricular wall.**

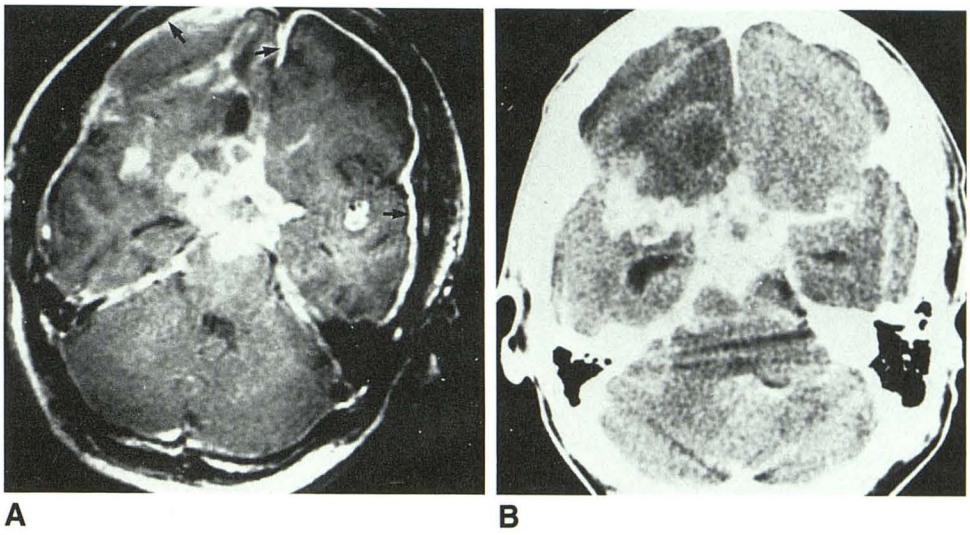

Fig. 2.—Case 7: Tuberculous meningitis.

***A*, GD-DTPA–enhanced SE 600/30 image shows multiple ring-enhancing granulomas in suprasellar and sylvian cisterns and curvilinear meningeal enhancement along convexity surface of brain (*arrows*).**

***B*, Meningeal enhancement at convexity surface is hardly detectable on postcontrast CT scan obtained 13 days before MR. Lentiform subdural fluid collection in right frontal convexity was caused by ventriculoperitoneal shunt procedure.**

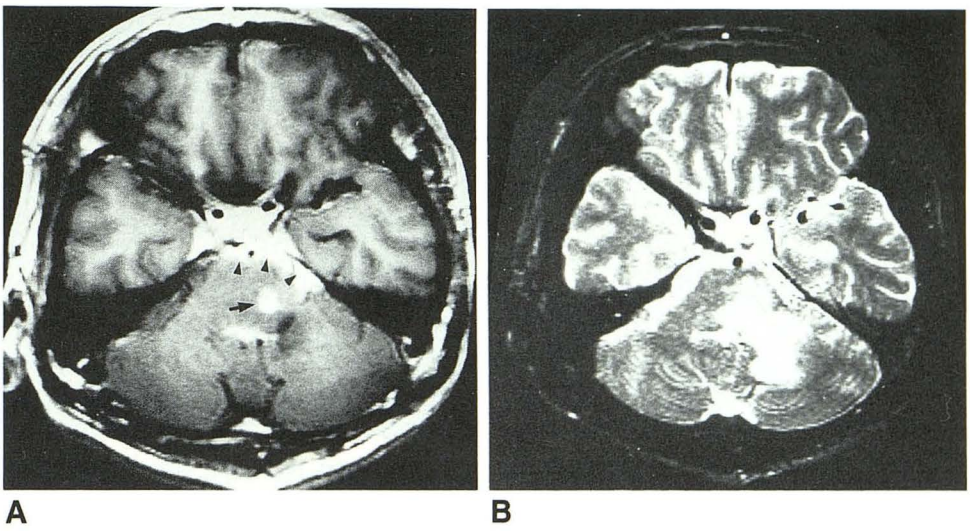

Fig. 3.—Case 3: Tuberculous meningitis.

***A*, Gd-DTPA–enhanced SE 500/30 image shows round, enhancing nodule (tuberculoma, *arrow*) in left side of pons and cisternal enhancement in prepontine and left cerebellopontine angle cisterns (*arrowheads*), as well as in suprasellar cistern.**

***B*, Gd-DTPA–enhanced SE 3000/80 image shows more extensive area of high signal intensity in pons and left side of cerebellum representing edema. Tuberculoma is not separated from surrounding edema. Lesion appears to be same as that seen on precontrast SE 3000/80 image (not shown).**

were readily identified in four patients on MR (Figs. 2 and 3), but in only three on CT. The granulomas usually were multiple, nodular or ring-shaped, and located at the basal cisterns and cortical areas of the brain. Some tiny nodules were seen only on MR. These enhancing lesions were demonstrated only on postcontrast T1-weighted images, and not on precontrast T1- and T2-weighted images. On postcontrast T2-weighted images, obtained in five selected patients, the enhancing granulomas were indistinguishable from surrounding edema (Fig. 3). Focal parenchymal signal abnormalities suggesting ischemia/infarct were identified in five patients on MR (Fig. 1) and in four on CT. These abnormalities were seen most often at the basal ganglia, and, less often, at the thalamus, midbrain, and deep periventricular white matter also. The precontrast T2-weighted image was the most sensitive in detecting these lesions. The hemorrhagic foci of high signal intensity on both precontrast T1- and T2-weighted images were demonstrated at the basal ganglia in two patients on MR (Fig. 1B), but in none on CT.

The five patients with bacterial meningitis included three with otogenous meningitis. In all three, MR showed abnormal signal intensity in the mastoid areas and localized contrast enhancement at the thickened tentorium along the ipsilateral petrous bone (Fig. 4). In one case of rhinogenous meningitis MR clearly demonstrated inflammation of the paranasal sinuses and adjacent thickened dural enhancement in association with subdural fluid collections. In addition, there were multiple areas of abnormal signal intensity suggesting ischemic infarction in the gyrus rectus bilaterally and in the right middle cerebral artery territory with gyral swelling (Fig. 5). These findings were demonstrated weakly or less clearly on CT. Abscesses observed in two patients (one in the cerebellum and the other in the deep parietal lobe) appeared as smooth, thick-walled rings of slightly high signal intensity with strong ring enhancement on the T1-weighted images, just like the CT appearance.

In the three patients with viral meningitis MR and CT findings were normal except for hydrocephalus in one patient.

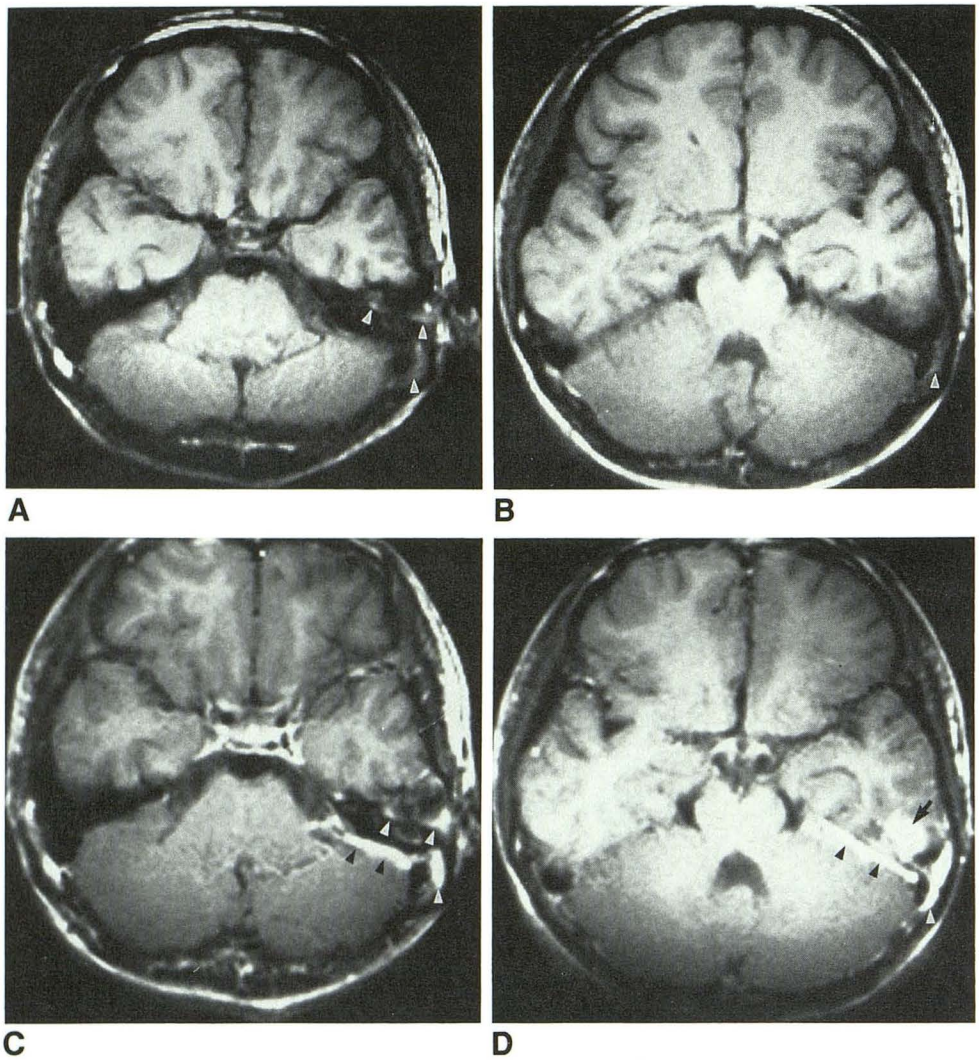

Fig. 4.—Case 10: Otogenous bacterial meningitis.

***A* and *B*, Precontrast SE 500/30 images. Variable degree of high signal intensity in left mastoid area represents mastoiditis (*arrowheads*).**

***C* and *D*, Gd-DTPA–enhanced SE 500/30 images show linear enhancement along tentorium adjacent to petrous bone (*black arrowheads*) and nodular enhancement just above petrous bone suggesting inflammatory mass (*arrow*), in addition to enhancement in area of mastoiditis (*white arrowheads*).**

Two patients had cryptococcal meningitis. Abnormal MR and CT findings in the basal ganglia in one suggested ischemic infarct. In the other patient normal MR and CT findings were seen during the convalescent period.

Hydrocephalus of varying degrees was identified equally well in 12 patients (six with tuberculous, four with bacterial, one with viral, one with cryptococcal meningitis) on both MR and CT. Periventricular edema was demonstrated clearly in seven of the 12 patients on T2-weighted images but in only five on both T1-weighted images and CT scans.

Associated findings included a subdural fluid collection complicated by a ventriculoperitoneal shunt procedure and interstitial edema around focal lesions. These were demonstrated equally well on MR and CT.

The MR and CT features of all patients are summarized in Table 1.

Discussion

A gross pathologic characteristic of tuberculous meningitis is a diffuse gray opacity in the leptomeninges owing to thick, gelatinous infiltrates around the base of the brain. Blood vessels running through the involved CSF spaces may be affected by the inflammatory exudate with resulting thrombosis and brain infarct. Interference with reabsorption of CSF produces communicating hydrocephalus [8, 18]. On CT, tuberculous meningitis is seen as varying degrees of contrast enhancement in the basal cisterns, communicating hydrocephalus, ischemia/infarct in the basal ganglia, and coexisting tuberculomas [1, 3, 4, 19]. In our series, ischemia/infarct in the basal ganglia was identified slightly more often on MR than on CT; hemorrhage was detected on MR only. The higher detection rate of MR might be due to the intrinsic higher sensitivity of MR and/or to lesions that developed during the interval between CT and MR (7 days each in cases 1 and 6; 9 days in case 2). Forty-three percent of ischemic infarcts may be complicated by a secondary hemorrhage at sometime during their course [20]. Inflammatory vasculitis, which may occur in any type of meningitis, is especially likely to produce such hemorrhagic infarcts [9].

Gd-DTPA–enhanced T1-weighted images unambiguously characterize the pathologic lesions, showing the abnormal blood/brain barrier and/or vascularity; in general, this pattern is mimicked on postcontrast CT, but the MR contrast en-

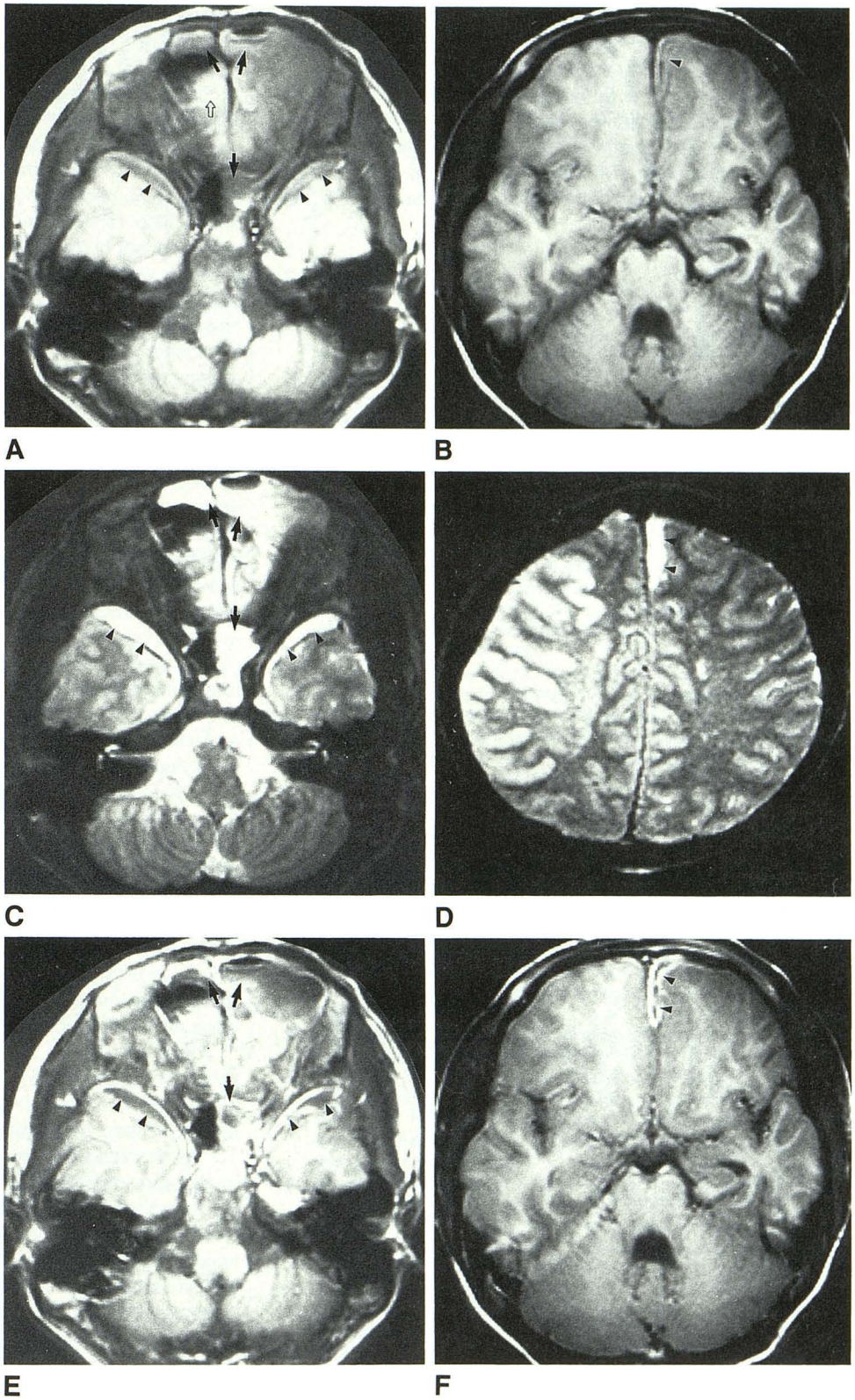

Fig. 5.—Case 9: Rhinogenous bacterial meningitis.

***A* and *D*, Precontrast SE 500/30 (*A* and *B*) and 3000/80 (*C* and *D*) images show inflammation of paranasal sinuses (*solid arrows*) and subdural fluid collections (*arrowheads*) in anterior temporal area bilaterally and in anterior interhemispheric fissure on left, associated with adjacent dural thickening. Localized high intensity in right paramidline frontal area (*open arrow*) on *A* presumably is due to artifacts from field inhomogeneity. Precontrast SE 3000/80 image (*D*) also shows edematous swelling of right frontoparietal gyri corresponding to middle cerebral artery territory, probably caused by ischemia/infarct secondary to vascular compromise. Focal areas in left centrum semiovale also appear involved.**

***E* and *F*, Gd-DTPA–enhanced SE 500/30 images. Thickened mucosae of paranasal sinuses (*arrows*) and thickened dura in area of subdural fluid collections (*arrowheads*) are densely enhanced. These abnormalities were not conspicuous on CT scans obtained 3 days before MR.**

hancement is more intense and MR is more sensitive [21–26]. In our series, MR imaging easily differentiated basal cisternal enhancement from signal-void vessels at the circle of Willis in a patient with CT findings of equivocal enhancement (case 2) and convexity meningeal enhancement from the inner table of the skull in another (case 7). Greater numbers of tuberculomas were seen on MR also. Better detection of these enhancing lesions by MR imaging might

TABLE 1: Summary of MR and CT Features in 18 Patients with Meningitis

Etiology/ Case No.	Age	Sex	MR/CT Findings (Location)							Associated Findings
			CT–MR Interval (days)	Meningeal Enhancement	Ischemia or Infarct	Hemorrhage	Granulomas	Hydrocephalus	Periventricular Edema	
Tuberculosis										
1	30	M	7	+/+ (SCC, SC, AC)	+/+ (BG, Th, Mb)	+/− (BG)	−/−	+/+	+/+	VP shunt ventriculitis
2	46	F	9	+/± (SSC)	+/− (BG)	−/−	−/−	+/+	+/−	–
3	29	M	6	+/+ (SSC, SC, AC, CPC)	−/−	−/−	+/+ (Po, Cbl, Th, In)	+/+	−/−	VP shunt
4	65	F	7	−/−	+/+ (BG)	−/−	+/+ (Hp, BG, FL, TL, OL)	+/+	+/+	–
5	24	F	5	+/+ (SSC)	−/−	−/−	−/−	+/+	−/−	–
6	41	M	7	+/+ (SC)	−/−	+/− (BG)	+/− (Po, TL)	+/+	+/−	–
7	39	F	13	+/+ (SSC, CM)	+/+ (BG)	−/−	+/+ (SSC, AC, CPC)	−/−	−/−	VP shunt
8	47	M	6	−/−	+/+ (BG, PW)	−/−	−/−	−/−	−/−	–
Bacterial										
9	14	M	3	+/− (CM, Fx, Te)	+/+ (FL, TL, PL)	−/−	−/−	+/+	−/−	PNS inflammation; SDF
10	21	M	5	+/+ (Te)	−/−	−/−	+/+ (TL)	−/−	−/−	Ear & mastoid inflammation
11	42	M	9	−/−	−/−	−/−	−/−	+/+	+/+	Cerebral abscess; ventriculitis
12	21	M	2	+/+ (CPC, Te)	−/−	−/−	−/−	+/+	−/−	Ear & mastoid inflammation; cerebellar abscess
13	12	M	7	+/− (Te)	−/−	−/−	−/−	+/+	+/+	Ear & mastoid inflammation
Viral										
14	45	M	5	−/−	−/−	−/−	−/−	−/−	−/−	–
15	44	F	1	−/−	−/−	−/−	−/−	+/+	−/−	–
16	58	F	5	−/−	−/−	−/−	−/−	−/−	−/−	–
Cryptococcal										
17	50	M	4	−/−	+/+ (BG)	−/−	−/−	+/+	+/+	–
18	34	F	6	−/−	−/−	−/−	−/−	−/−	−/−	VP shunt

Note.—+ = present; ± = equivocal; − = absent; VP = ventriculoperitoneal; SSC = suprasellar cistern; SC = sylvian cistern; AC = ambient cistern; BG = basal ganglia; Th = thalamus; Mb = midbrain; CPC = cerebellopontine angle cistern; Po = pons; Cbl = cerebellum; In = insula; Hp = hypothalamus; FL = frontal lobe; TL = temporal lobe; OL = occipital lobe; CM = convexity meninges; PW = periventricular white matter; Fx = falx; Te = tentorium; PL = parietal lobe; PNS = paranasal sinuses; SDF = subdural fluid collection.

have been related to the progression of the disease process during the interval between CT and MR (9 days in case 2 and 13 days in case 7), but it seems more likely to have resulted from the intrinsic higher sensitivity of MR and Gd-DTPA.

Recently, Mathews et al. [27] reported an experimental study on Gd-DTPA–enhanced MR imaging in bacterial meningitis. They found that while precontrast MR was not helpful in identifying meningitis, Gd-DTPA–enhanced MR images were superior to postcontrast CT scans, not only in the detection of meningeal involvement but also in the identification of complications. MR is also superior in its ability to detect extracerebral fluid collections since it is free of bony artifacts adjacent to the inner table of the skull. Even small amounts of subdural fluid are visible as crescentic fluid collections along the surface of the brain [11]. While CT is often equivocal, MR may be able to differentiate between benign subdural effusions and infected subdural empyemas by virtue of the shortened T1 relaxation times of purulent fluid in comparison with CSF [28]. Subdural effusions are low-protein collections that, therefore, are isointense relative to CSF, while empyemas are more proteinaceous and have intensities different from that of CSF [14–16]. On T1-weighted images, empyemas are hyperintense relative to CSF, while subdural effusions are isointense relative to CSF [14]. We speculate that the subdural fluid collections seen in case 9 (Fig. 5) were empyemas rather than simple effusions because they were hyperintense relative to CSF and surrounded by a densely enhancing wall on T1-weighted images. However, this was not surgically verified. Localized enhancement of thickened dura adjacent to the inflamed paranasal sinuses or petrous bone on MR was considered to be characteristic of bacterial meningitis secondary to rhinogenous or otogenous infection. Gd-DTPA enhancement was not visible routinely in the dura, including the falx cerebri and tentorium. Kilgore et al. [29] reported that the falx cerebri and tentorium cerebelli are normally enhanced after Gd-DTPA administration in approximately half the patients. In six patients in our series, dural enhancement was normal: the dura was not thickened; it was enhanced in a short, linear fashion; there were no adjacent abnormal findings; and it was easily differentiated from pathologic dural enhancement.

In summary, our results indicate that although precontrast T2-weighted images were the most sensitive in delineating ischemia/infarct and edema, they were not as specific as Gd-DTPA–enhanced T1-weighted images and postcontrast CT scans in defining the diffuse active inflammatory process of the meninges and focal lesions precisely. The precontrast T1-weighted image proved even more difficult to interpret. It not only failed to demonstrate the active inflammatory process of the meninges and the focal lesions but it also showed the ischemia/infarct and edema as a subtle low-intensity signal. However, precontrast T1-weighted imaging is necessary because it helps in the detection of subacute hemorrhage. Therefore, both precontrast T1- and T2-weighted imaging and Gd-DTPA–enhanced T1-weighted imaging are considered necessary in the evaluation of the patient with suspected meningitis. All the possible abnormalities—including pericranial lesions (paranasal sinusitis and otitis media), meningeal inflammation, hydrocephalus, ischemia/infarct, hemorrhage, granuloma, abscess, and surrounding edema—can be identified more clearly on MR with the above sequences than on CT. The major role for Gd-DTPA in meningitis likely will be the identification of active blood/brain barrier disruption and increased vascularity, possibly facilitating the detection of the disease process at an early stage when it may not be detected on CT. Thus, if Gd-DTPA is used, MR appears to be superior to CT in the evaluation of leptomeningitis.

REFERENCES

1. Enzmann DR, Norman D, Mani J, Newton TH. Computed tomography of granulomatous basal arachnoiditis. *Radiology* **1976**;120:341–344
2. Zimmerman RA, Patel S, Bilaniuk LT. Demonstration of purulent bacterial intracranial infections by computed tomography. *AJR* **1976**;127:155–165
3. Cockrill HH, Dreisbach J, Lowe B, Yamauchi T. Computed tomography in leptomeningeal infections. *AJR* **1978**;130:511–515
4. Casselman ES, Hasso AN, Aschwal S, Schneider S. Computed tomography of tuberculous meningitis in infant and children. *J. Comput Assist Tomogr* **1980**;4:211–216
5. Bydder GM, Steiner RE, Young IR, et al. Clinical NMR imaging of the brain: 140 cases. *AJNR* **1982**;3:459–480
6. Brant-Zawadzki M, Davis PL, Crooks LE, et al. NMR demonstration of cerebral abnormalities: comparison with CT. *AJR* **1983**;140:847–854
7. Bradley WG, Waluch V, Yadley RA, et al. Comparison of CT and MR in 400 patients with suspected disease of the brain and cervical spinal cord. *Radiology* **1984**;152:695–702
8. Zimmerman RA, Bilaniuk LT, Sze G. Intracranial infection. In: Brant-Zawadzki M, Norman D, eds. *Magnetic resonance imaging of the central nervous system*, 1st ed. New York: Raven, **1987**:235–257
9. Brant-Zawadzki M, Kucharczyk W. Vascular disease: ischemia. In: Brant-Zawadzki M, Norman D, eds. *Magnetic resonance imaging of the central nervous system*, 1st ed. New York: Raven, **1987**:221–234
10. Sze G. Infections and inflammatory diseases. In: Stark DD, Bradley WG, eds. *Magnetic resonance imaging*, 1st ed. St. Louis: Mosby, **1988**: 316–343
11. Davidson HD, Steiner RE. Magnetic resonance imaging in infections of the central nervous system. *AJNR* **1985**;6:499–504
12. Schroth G, Kretzschmar K, Gawehn J, Voigt K. Advantage of magnetic resonance imaging in the diagnosis of cerebral infections. *Neuroradiology* **1987**;29:120–126
13. Lee SH. Infectious diseases. In: Lee SH, Rao K, eds. *Cranial computed tomography and magnetic resonance imaging*, 2d ed. New York: McGraw-Hill, **1986**:557–600
14. Sze G, Zimmerman RD. Magnetic resonance imaging of infections and inflammatory diseases. *Radiol Clin North Am* **1988**;26:839–859
15. Becker RD, Zimmermann RD, Sze G, et al. MR of subdural empyema and other extraaxial inflammatory lesions (abstr). *AJNR* **1987**;8:940
16. Zimmerman RD, Becker RD, Devinsky O, et al. Magnetic resonance imaging features of cerebral abscesses and other intracranial inflammatory lesions. *Acta Radiol [Suppl]* (Stockh) **1986**;369:754
17. Gupta RK, Jena A, Sharma A, et al. MR imaging of intracranial tuberculomas. *J. Comput Assist Tomogr* **1988**;12:280–285
18. Parker JC, Dyer ML. Neurologic infections due to bacteria, fungi, and parasites. In: Davis RL, Robertson DM, eds. *Textbook of neuropathology*. Baltimore: Williams & Wilkins, **1985**:632–703
19. Whelan MA, Stern J. Intracranial tuberculoma. *Radiology* **1981**;138:75–81
20. Hornig CR, Dorndorf W, Agnoli AL. Hemorrhagic cerebral infarction—a prospective study. *Stroke* **1986**;17:179–185
21. Grossman RI, Joseph PM, Wolf G, et al. Experimental intracranial septic infarction: magnetic resonance enhancement. *Radiology* **1985**;155: 649–653
22. Felix R, Schorner W, Laniado M, et al. Brain tumors: MR imaging with gadolinium-DTPA. *Radiology* **1985**;156:681–688
23. Brant-Zawadzki M, Berry I, Osaki L, Brasch R, Murovic J, Norman D. Gd-DTPA in clinical MR of the brain: 1. Intraaxial lesions. *AJNR* **1986**;7: 781–788
24. Berry I, Brant-Zawadzki M, Osaki L, Brasch R, Murovic J, Newton TH.

Gd-DTPA in clinical MR of the brain: 2. Extraaxial lesions and normal structure. *AJNR* **1986**;7:789–793

25. Schorner W, Laniado M, Niendorf HP, Schubert C, Felix R. Time-dependent changes in image contrast in brain tumors after gadolinium-DTPA. *AJNR* **1986**;7:1013–1020
26. Davis PC, Hoffman JC, Malko JA, et al. Gadolinium-DTPA and MR imaging of pituitary adenoma: a preliminary report. *AJNR* **1987**;8:817–823
27. Mathews VP, Kuharik MA, Edwards MK, D'Amour PG, Azzarelli B, Dreesen RG. Gd-DTPA-enhanced MR imaging of experimental bacterial meningitis: evaluation and comparison with CT. *AJNR* **1988**;9:1045–1050
28. Brant-Zawadzki M, Kelly W, Kjos B, et al. Magnetic resonance imaging and characterization of normal and abnormal intracranial cerebrospinal fluid (CSF) spaces: initial observations. *Neuroradiology* **1985**;27:3–8
29. Kilgore DP, Breger RK, Daniels DL, Pojunas KW, Williams AL, Haughton VM. Cranial tissues: normal MR appearance after intravenous injection of Gd-DTPA. *Radiology* **1986**;160:757–761